Vol. 20, No. 1 (2021) 87-96
Revista Mexicana de Ingeniería Química

Effect of the concentration of glycerin in the performance of chitosan membranes utilized in aqueous phase permeation

Efecto de la concentración de glicerina en el desempeño de membranas de quitosano utilizadas en permeación en fase acuosa

J.A. Galicia-Aguilar[1]*, M. López-Badillo[1], M.A. García-Castro[1], J.L. Varela-Caselis[2], C. Solís-Martínez[1], J. Ortega-Pérez[1]

[1]*Benemérita Universidad Autónoma de Puebla, Facultad de Ingeniería Química, 18 sur y San Claudio, Ciudad Universitaria, C. P. 72570, Puebla, Pue., México.*

[2]*Benemérita Universidad Autónoma de Puebla, Centro Universitario de Vinculación y Transferencia Tecnológica, Prolongación de la 24 sur y Av. San Claudio, Ciudad Universitaria, C. P. 72570 Puebla, Puebla, México.*

Received: January 19, 2020; Accepted: April 30, 2020

Abstract

We have carried out the synthesis of a series of chitosan-based membranes by casting solution method. The membranes were synthesized from commercial chitosan and glycerin as a plasticizer, varying the concentration of glycerin to determine the concentration that allows the formation of membranes with the best physicochemical properties to retentate permeating test molecules. Formed membranes were cross-linked with sulfuric acid, and tested in the permeation of sodium chloride, saccharose and a whey protein. The physicochemical characteristics of the membrane were evaluated by the water swelling factor, viscous molecular weight and DSC. The passage of the tested molecules through the membrane and other characteristics were modified with glycerin content in the forming solution.

Keywords: Chitosan, membrane, glycerin, cross-linking, permeability.

Resumen

Llevamos a cabo la preparación de una serie de membranas a base de quitosano mediante el método de evaporación de la solución. Las membranas fueron formadas a partir de quitosano comercial y glicerina como plastificante, variando la concentración de glicerina con objeto de determinar la concentración que permita la formación de membranas con las mejores características fisicoquímicas para retener las moléculas estudiadas. Las membranas formadas fueron reticuladas con ácido sulfúrico, y evaluadas en la permeación de cloruro de sodio, sacarosa y un lactosuero. Las características fisicoquímicas de las membranas fueron evaluadas mediante el factor de hinchamiento en agua, el peso molecular viscoso y DSC. El paso de la molécula en evaluación a través de la membrana y otras características fueron modificadas con la concentración de glicerina usada en la solución formante.

Palabras clave: Quitosano, membrana, glicerina, reticulación, permeabilidad.

1 Introduction

Membrane separation technology has attracted the attention to solve the growing demand of high-quality products thanks to its high performance in fluid phase separation (Scott, 1995) (Shahidi *et al*., 1999). This technology has low energetic and process requirements as well as low environmental impact making it suitable to separate a wide spectrum of fluids. Polymer materials have increased the applicability of the technology due to the facility to form membranes of a wide variety of porous structures. In fact, the membrane is designed as a function of the separation requirements of the fluid. Thereby, microfiltration, nanofiltration, pervaporation (Han *et al*., 2014) forward and inverse osmosis are outlined by structural characteristics of the membranes where separation is carried out by size exclusion of the penetrants.

* *Corresponding author. E-mail*: jose.galicia@correo.buap.mx
https://doi.org/10.24275/rmiq/Bio1198
issn-e: 2395-8472

Process like the inverse osmosis are utilized to desalinate sea water; the purification of biotechnological products, such as pharmaceutics or therapeutics, are carried out from ultrafiltration or microfiltration (van Reis & Zydney, 2007). It is worth mentioning that conventional process exhibit disadvantages due to high operating costs or high quantity of separation stages, that cannot be outperformed (González-Valdez *et al*., 2014). Instead, the technological development was oriented to membrane process like ultrafiltration, that does not requires chemical additives or heat, which guaranties the integrity of the raw mater, increasing the applicability of the technology (Carmona-Gómez *et al*., 2018).

Considering polymer materials to train membranes, the biopolymers such as chitosan (Xin-Ping *et al*., 1996) are preferable over synthetic ones due to its biodegradability. Chitosan is a polysaccharide derived from partial deacetylation of chitin, containing $\beta(1 \rightarrow 4)$ glycosidic 2-amino-2-deoxy-d-glucopyranose units, where the amino groups of chitosan allow its solubility in weak acidic media (Sivashankari & Prabaharan , 2017). Chitosan based membranes can be utilized to separate several solutes in food industry (Chaudhary *et al*., 2011), pharmaceutics, medical use in drug administration, orthopedics, dentistry and cosmetic encapsulation (Tharanathan, 2013). When chitosan is utilized to form membranes, its permeability is affected by factors such as the swelling factor ($S\,f$), the deacetylation degree (DD) and the molecular weight (MW). This variables have been studied in the extraction of chitosan from chitin, and is well accepted that MW is not affected by DD, but the $S\,f$ increases when MW decreases (Xi-Guang *et al*., 2002). It is worth notice that permeability is strongly linked to those variables that fall upon the membrane performance. In fact, the −OH groups gives the hydrophilic character to chitosan (Zhu *et al*., 2015), making the swelling of the membrane in aqueous medium possible.

Chitosan has been recommended for several applications, particularly to train the chitosan as a membrane, a plasticizer is necessary in order to increase the flexibility. The plasticizer reduces the intermolecular forces, smoothing the strength of the polymeric membranes, allowing the increase of the chain mobility, and performing its mechanical properties (Srinivasa *et al*., 2007). Some plasticizers reported in literature includes glycerin, sorbitol, polyethylene glycol, which are used in chitosan membranes preparation. For example, when glycerin is used as plasticizer, the chain flexibility increases compared to sorbitol or PEG. Different research has demonstrated that glycerin is an efficient plasticizer to chitosan, because allow to modify its macroscopic properties. It has been reported that chitosan membranes with 25% wt glycerin increases its ductility, hydrophile properties and 40% of elongation at break (Epure *et al*., 2011). The interaction between glycerin and chitosan impacts in the increase of the free volume, causes a strong decrease of the glass transition temperature (Tg), increase in the elasticity and permeability to water vapor (Rivero *et al*., 2016). Chitosan and glycerin interactions are evidenced by −CH and −OH groups. It is reported that increasing glycerin concentration increases the −OH groups to interact with chitosan (Liu *et al*., 2013). Another example of plasticizer is the use of lipids, added to biodegradable films based on chitosan, used as additives to modify the mechanical properties and strengthen its water barrier. For this, it has been reported the naturals extracts as *Moringa oleifera* leaf (Núñez-Gastélum *et al*., 2018) and lemon essential oil (Ramos-García *et al*., 2017).

Biopolymers exhibit a high sensibility to humid environments due to its hygroscopic nature. For that, the use of chitosan membranes involves a technological challenge to operate in aqueous phase, due to the plasticized effect of the water molecules or the erosion of the functional groups of the polymer, modifying the physical properties of the membrane (Bergo *et al*., 2012). Besides that, to limit the swelling of the membrane and to increase its mechanical resistance, the membranes are modified cross-linking (Sajjan *et al*., 2015). The cross-link reaction is the most viable way to reinforce the chemical structure of chitosan based membranes and to limit the swelling factor, due to the formation of links between the polymeric chains with the consequently delimitation of the chain mobility and increase of the packing density. The cross-linkers reported for chitosan includes sulfuric acid, poly triphosphate, glutaric aldehyde, diglycil glycol ether. In the cross-linking reaction with sulfuric acid, the formed membrane is immersed in a sulfuric acid solution, where sulfate anions (SO_4^{-2}) interacts with the amine groups (NH_2) of chitosan to protonate (NH_3^+) and link the polymeric chains (Cui *et al*., 2008) (Marques *et al*., 2016). This means that sulfuric acid cross-link the polymeric chains by ionic interactions. In the same way has been reported the chitosan cross-linking by short wave UV radiation in edible films (López-Díaz *et al*., 2018).

The permeability of the membrane is also a function of the permeating molecule. The permeability take place according to the molecular size of the penetrant, inter alia. Thus, big size molecules are retained in one side of the membrane while biggest ones are retained (Bullón *et al*., 2001). The molecular affinity of the membrane to the penetrant have also a direct influence over the membrane permeability, and chitosan membranes exhibit high affinity toward organic molecules (Kolesnyk, *et al*., 2020). In order to obtain membranes useful for the aqueous phase permeation, in this work a series of chitosan membranes were trained. From glycerin as plasticizer at different concentrations keeping constant the cross-linker concentration and immersion time. The membranes were characterized and evaluated in NaCl, saccharose and whey protein permeation in order to determine the effect of the cross linked chitosan and the plasticizer over the structure of the membrane.

2 Materials and methods

2.1 Reactive

Chitosan low molecular weight (98%, Sigma-Aldrich), acetic acid glacial (98%, Meyer), sodium hydroxide (98%, Meyer), sulfuric acid (98.4% J.T. Baker), glycerin (99.59% QCA).

2.2 Training membranes

Chitosan powder was dissolved in a 0.1 M acetic acid solution at 1%w/v, 90 °C and magnetic stirring for 24 hours. Then, the solution was filtrated, and glycerin was added and keep stirring for 4 hours more at 90 °C. Flat membranes were formed with 20 mL of the chitosan solution at different glycerin concentration in a 10 cm diameter Petri dish.

Table 1. Synthesized samples.

Sample	Glycerin,%w/v	Sf	Thickness, mm
M1	0.1	1.28	0.02625
M2	0.3	1.52	0.05775
M3	0.5	2.10	0.10325
M4	0.7	2.39	0.2465

*All the samples were cross-linked in a 0.5M sulfuric acid solution

Finally, the solvent was slowly evaporated at room temperature for 24 hours and 60 °C for 72 hours. Table 1 indicate the glycerin content of each membrane.

2.3 Chemical cross-linking

The formed membranes were immersed in a 0.5 M sulfuric acid solution for 24 hours to cross link the polymeric chains. After this, membranes were washed several times and neutralized in a 2 M sodium hydroxide solution for 5 minutes. Finally, the membranes were washed until pH 7 was reached. The codification for the synthetized samples is indicated in Table 1.

2.4 Characterizations

The viscosity of chitosan in a 0.1M acetic acid (CH_3COOH) solution was determined in an Ubbelohde viscometer at 25 °C, and the relative viscosity (η_{rel}) was calculated from Equation 1:

$$\eta_{rel} = \frac{\eta_{sol}}{\eta_{dis}} \tag{1}$$

where η_{sol} and η_{dis} are the solution and dissolvent experimental viscosities, respectively. The average molecular weight ($\overline{M}_w$) of the chitosan was calculated from the Mark-Houwink-Sakurada (Equation 2), in which the constants are a function of the degree of deacetylation (DD), and were calculated as proposed by Wang *et al*. (1991), Equations 3 and 4.

$$[\eta] = K\left(\overline{M}_w\right)^a \tag{2}$$

$$K = 1.64 * 10^{-30} * DD^{14} \tag{3}$$

$$a = -1.02 * 10^{-2} * DD + 1.82 \tag{4}$$

where constant a is related to the solvent quality and K is the intrinsic viscosity. To determine the swelling factor (Sf), a dry cross-linked membrane was immersed in an excess of bidistilled water for 24 hours. The Sf was calculated as indicated by Equation 5. The experimental data were carried out by three in order to assure the reproducibility.

$$Sf = \frac{W_s - W_d}{W_d} \tag{5}$$

where W_s and W_d is the weight of the swollen and dry membrane, respectively.

The membrane thickness was measured to the cross-linked samples with a micrometer Metrology EM-9001N. The thickness measurements were carried

out in several parts of the membrane, and the reported data is the average of 20 measurements.

The functional groups where identified by FTIR – ATR in a Perkin Elmer FTIR spectrometer. Hence, the DD was calculated from the absorption ratio between the tertiary amine at 1376 cm^{-1} and secondary amine at 1571 cm^{-1}, according to Equation 6:

$$DD(\%) = 100 - 31.94\frac{A_{1376}}{A_{1571}} - 12.2 \qquad (6)$$

The glass transition temperature of the cross-linked membranes was measured in a Mettler Toledo Star System DSC operating at 30 ml/min of N_2 flux. The measurements were carried out in two steps. In the first one, heating from 30 – 150 °C and 10 °C/min. The second one was carried out from 30-200 °C at a heating rate of 40 °C/min.

2.5 *Permeability*

The cross-linked membranes were utilized to determine the permeability in liquid phase in a batch system, operating at 25 °C. The device consists of two sections joined by a flange where the membrane is hold by a porous support. The mass transfer area is 4 cm^2.

The permeation device was placed in horizontal position, keep at ambient temperature and magnetically stirred in both cameras. Three model solutions were utilized to characterize the membrane permeability, placed in one side of the device, and the collecting camera was filled with bidistilled water in all the cases. The first solution was 1%wt NaCl where the concentration was determined by conductimetry in the first five hours. The mass transport through the membrane can be described by a semiempirical model, in which the mass balance for the system relates the flow of permeating molecules normalized by the membrane area, in the direction of diffusion (x) to accumulation in the receiving area. The model is based in the Fick's law for the diffusivity and Henry's law for the solubility.

Table 2. Whey protein composition.

Parameter	measuring range
Fat	0.01 - 25%
Density	1000 - 1150 kg/m^3
Protein	2 - 7%
Lactose	0.01 - 20%
Salt	0.4 - 4%

The upstream concentration must be constant over time (for this, a high concentration is utilized), then the mass balance can be solved with the following boundary conditions: $C(0,t) = C_0$ and $C(L,t) = C_i$. Thus, the permeability can be calculated as indicated in Equation 7:

$$P = \frac{276\ V\ L}{A\ TC_0} * \frac{dC}{dt} \qquad (7)$$

where V is the chamber volume (cm^3), L the membrane thickness (cm), A the effective membrane area (cm^2), T the temperature (K), C_0 the initial concentration (mol/L). The variation of the concentration as a function of time was determined from the slope of the concentration at initial times. In the reception chamber, the concentration of the solute was measured at the beginning and end of the permeation experiment.

The second solution was a 1% saccharose utilized to determine the passage of a bigger molecule through the membranes. Thus, the variations in concentration were quantified in both sides of the membrane by polarimetry at 24, 48 and 72 hours.

The third solution was a 1% whey protein solution where the concentration was determined in a Lactoscan Milkotronic Ltd, after 72 hours of experimentation. The whey protein composition was determined at the beginning of the test and the ranges reported by the lactoscan are resumed in Table 2.

3 Results and discussion

Concerning the chitosan reactive, the molecular weight and the DD are fundamental properties of the polymer determining the applicability. From the FTIR-ATR spectra and Equation 6, the DD of the commercial chitosan was calculated as 80.26%. The acetylene groups make the structure stiff by steric hindrance; by removing this groups, the ionizable NH_2 stay exposed becoming the molecule soluble in light acidic aqueous solution, and then is considered chitosan (Zhao Wang *et al*., 2006). With the calculated constants ($K = 7.54e^{-4}$ mL/g and a = 1.001) from the FTIR-ATR spectra, the molecular weight is 8,674 g/mol, which is considered as low in the literature. Once evaporated the solvent the membranes are removed from the Petri dish. The uncross-linked chitosan membrane can be dissolved when immersed in water.

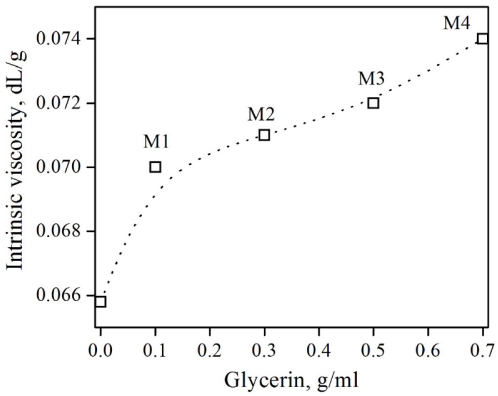

Fig. 1. Viscosity of the chitosan − glycerin dissolutions.

However, after immersed in the cross-linking solution, the membranes can no longer dissolve due to the formation of ionic interactions between polymer chains. In the same way, the viscosity of the chitosan solution can be measured only before the cross-linking reaction. The viscosity increases as glycerin is added to the dissolution as exhibited in Figure 1. The viscosity of the polymer in solution is directly related to its molecular weight. However, the observed increase is better related to the viscosity of the mixture and reflects a uniform integration of the chitosan and glycerin, assuring uniform properties in the membrane. Consequently, the formed membranes are no brittle, rather the pliability and malleability increases adding glycerin.

The membranes exhibit a notably increase in the thickness, associated to the glycerin addition reported in Table 1. The plasticizer do not creates chemical bonds rather increases the interchain space due to the reduction of the interaction van der Waals attractive forces polymer − polymer, increasing the free volume (Godwin, 2011). The free volume is a measure of the internal space available in the membrane. As the free volume increases, a wider space available allow the chain movement, making the polymer network more flexible.

3.1 Swelling factor (S f)

The calculated swelling factor in water is reported in Table 1. The $S\,f$ increases as glycerin concentration increases in the membrane composition. The plasticizer has three −OH polar groups, which interacts with the polymer due to its cationic polyelectrolyte nature. Hence, a polar part of the glycerin interacts with the chitosan, while the rest of the polar part contributes to the free volume and to the hydrophilic character of the resulting polymer, according to the plasticizer theory (Buszard, 1984). Therefore, at low plasticizer concentration, the polymer-plasticizer interactions are dominant while at high plasticizer concentration, the plasticizer−plasticizer interactions are dominant allowing the swelling of the membrane (Godwin, 2011). It is worth notice that the highest $S\,f$ is a little more than two, indicating a limited $S\,f$ compared to hydrogels or chitosan mixed with hydrophilic polymers, possibly due to the cross-linking degree of the membranes which counteracts the osmotic forces described previously (Bocourt-Povea *et al*., 2008) (Chaudhary *et al*., 2011).

3.2 Thermal analyses

Membranes were analyzed by Differential Scanning Calorimetry (DSC). A first heating was carried out at 10 °C/min from 25−120 °C, to eliminate low boiling point solvents. Figure 2a) shows the thermograms where a wide absorption zone at low temperatures indicates the water evaporation. This endothermic zone associated to the water evaporation indicates the water retention by the membrane. A second heating at 40 °C/min from 30−200 °C allows to identify the structural transformations in the temperature range. Figure 2b) exhibit the thermogram where the different transitions can be observed, being the higher Tg in membranes lower than Tg of chitosan (Tg = 151.5 °C) except for sample M4. This is due to the plasticizer penetration to the bundles of the polymer, changing the structure from glassy to rubbery (Buszard, 1984).

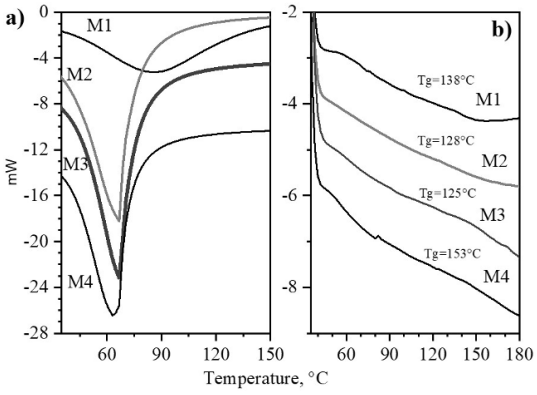

Fig. 2. DSC thermogram: a) first heating and b) second heating of the membranes.

It is worth notice that the cross link prevents the reduction of the Tg, as reported in plasticized uncross linked membranes, which reports the Tg in the range from 20 to 93 °C, depending of the glycerin concentration (Rivero *et al*., 2016). The several thermal events in the membranes are indicating a heterogeneous structure from the cross-linking reaction, because the thickness of the membrane prevents the cross-linker from reaching the deeper sites. These results agree the literature reports where chitosan Tg is a function of molecular weight and the deacetylation degree (Neto *et al*., 2005). However, there are two facts in a thermal characterization of a polymer; the first one, is that thermostable polymers do not exhibit glass transition temperature. Then, formed membranes do not form covalent links in the cross-linking reaction. The second fact is related to the several thermal events, revealing the existence of polymeric chains of several size.

3.3 Permeability

3.3.1 NaCl permeation

To determine the conductivity variations as a function of time, the electrode was fixed to the pure water camera. Figure 3 shows that conductivity increases suddenly in the first hours, with a slightly different slope for each membrane. Conductivity reach an equilibrium concentration between cameras depending of the membrane characteristics. It is worth notice that samples M2 and M4 exhibit the best trend to equilibrium between the cameras.

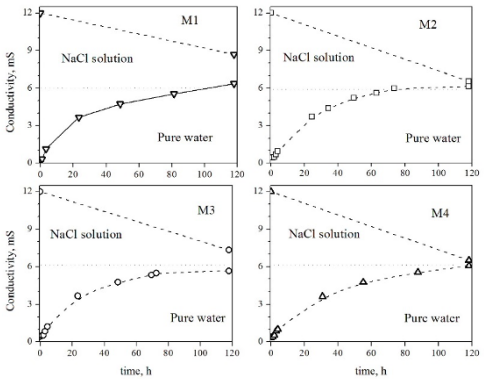

Fig. 3. Conductivity variation as a function of time in the membrane cell permeation.

Table 3. Calculated kinetic constants from concentration experiments.

Sample	Lagergren model		
	k_1 (1/h)	C_1^{cal} (mol/L)	R^2
M1	0.0250	5.7190	0.9874
M2	0.0378	5.9576	0.9982
M3	0.0412	5.1360	0.9968
M4	0.0274	5.7334	0.9995

3.3.1.1 Kinetic analysis

The variation of the concentration as a function of time was analyzed with the pseudo first order model of Lagergren (Ho & McKay, 1998). The lineal form of the kinetic model is indicated by:

$$\ln \frac{C_e - C}{C_R} = \ln \frac{C^{calc}}{C_R} - k_1 * t \tag{8}$$

where C_e, C, C^{calc} and C_R are the concentration at equilibrium, at time t, calculated from the model and reference (1 mol/L), respectively (mol/L) and k_1 is the rate constant of pseudo-first order (h^{-1}). It is worth notice that the linearized form of equation involves the logarithm in both sides. The division between CR makes the argument of the logarithms in equation 8 the ratio of two variables having the same units, as indicated by Matta, to solve the dimensional analysis (Matta *et al*., 2011).

Table 3 resumes the calculated values for the kinetic constants from the first order model. The correlating coefficient (R^2) was used as fitting parameter, indicating a high response with the first order model. Worth mentioning that first order model involves two zones, a first one indicating a rapid increase, in this case, of the concentration in the water camera, and a second one, forming a plateau associated with an equilibrium zone, as exhibited in Figure 3. Finally, the rate of passage of the molecule through the membrane is affected by the increase of the thickness, as observed by other authors (Mu *et al*., 2019).

3.3.1.2 NaCl permeability

From the solute concentration, the permeability was calculated as indicated in Equation 7. At low experimentation time, a transitory state was observed, but when time increases a steady state is identified where the slope determine the variation of concentration with the time.

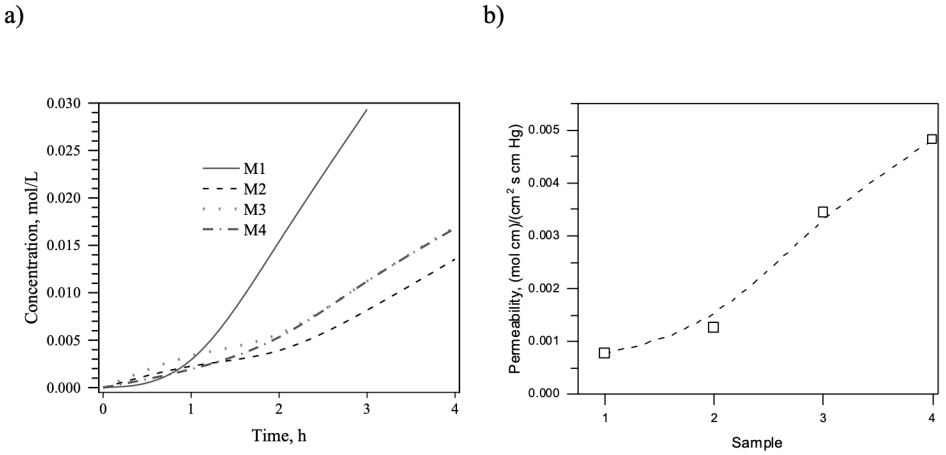

Fig. 4. a) Variation of the concentration as a function of time and b) calculated permeability of the membranes with NaCl as permeating molecule.

Figure 4a shows the data of concentration as a function of time for the synthesized membranes. The permeability was plotted in Figure 4b. It is worth notice that the permeation time is high enough to reach the steady state, once this, the concentration increases linearly with time, exhibiting a different rate as a function of nominal glycerin concentration. Then, membrane M4 exhibit the highest permeability, which agrees with the highest swelling factor, hence it is possible that the increase of the chain separation allows to increase the membrane permeability.

3.3.2 Saccharose permeation

Figure 5 shows the variation of the saccharose concentration as a function of time for the membranes in both cameras. The concentration varies with the glycerin concentration utilized in the membrane preparation, being membrane M1 and M4 the samples with lower oscillations in the measured concentration. Sample M1 exhibit a sharp decrease in concentration in the camera charged with saccharose and a low increase in the water camera, indicating that the penetrating molecule cannot diffuse through membrane, remaining possibly adsorbed in the membrane. With sample M4 the concentration decreases to reach an equilibrium between the cameras, indicating that the membrane has higher spaces to allow the mass transfer. This result indicates that the cavity size in the membrane increases with glycerin addition to the membrane. Finally, the saccharose permeation is slower than NaCl permeation, due to the difference in molecular size of the studied molecules.

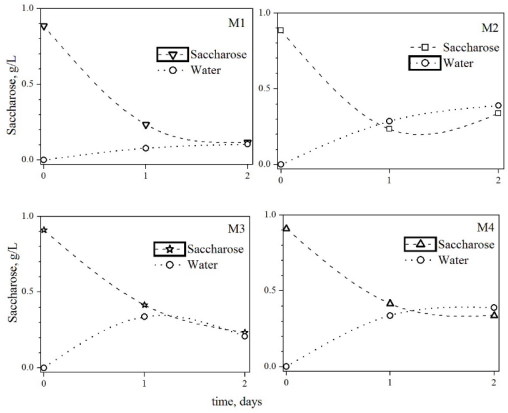

Fig. 5. Saccharose concentration data as a function of time: a) M1, b) M2, c) M3 and d) M4.

3.3.3 Whey protein permeation

The whey protein was diluted at 10% v/v with water and introduced to the permeation cell. The cell was tightly closed and remained at this condition for 72 hours, then the whey protein analyzed in both cameras. Figure 6 exhibit the concentration of the components of the whey protein in each side of the membrane. The camera I charged with water was free of any whey protein component (Figure 6a), excluding membrane M4, where parameters such as density, lactose and salt were increased. Figure 6b exhibit the composition of the camera II charged with the whey protein, where the grass content increases in all the membranes. Parameters such as density, lactose, salt and protein increase according to the type of membrane.

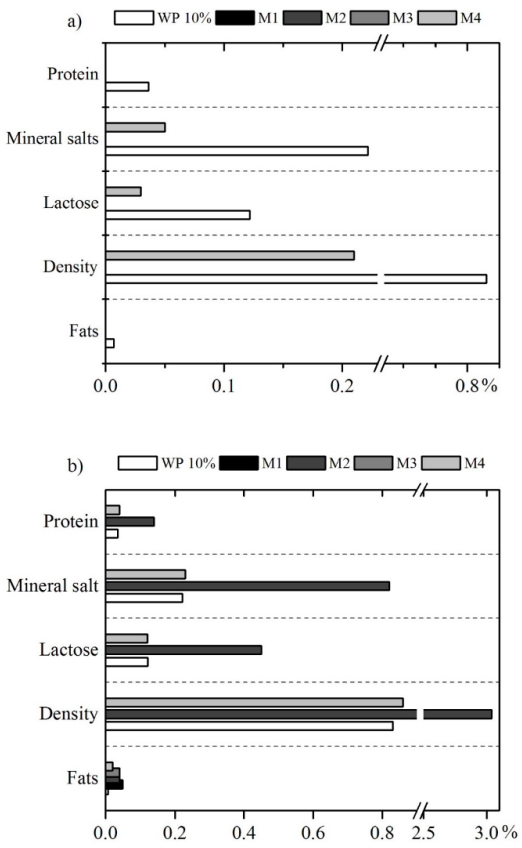

Fig. 6. Comparative composition of the whey protein determined by Lactoscan, and after 72h of contact with the membrane, a) Camera I charged with water and b) Camera II charged with whey protein.

For example, membrane M2 and M4 exhibit higher levels in the parameters mentioned above, but membrane M1 and M3 increases its level just for the grass content. Since in camera I those parameters were not detected, only water goes through the membrane, consequently, the density, lactose content, salt and protein are increased compared to the reference whey protein.

Finally, it is worth mentioning that whey protein has the lowest rate of passage of through the membrane of the tested molecules. This could be due to the complexity of the whey protein composition and the size of the molecules due to steric factors (Perez-Escobar *et al*., 2020). Similar trends have been reported for bovine serum albumin, which is slowest to lower size penetrants (Chen *et al*., 2016) (Chen *et al*., 2002).

Conclusions

Flat membranes from chitosan with different glycerin concentrations were formed by solution evaporation method. Membranes were cross-linked and consequently, they were insoluble in any solvent. However, the hydrophilic character was modified by the glycerin content utilized in the membrane formation, as revealed the swelling factor. The membranes exhibit a heterogeneous structure as revealed the multiple glass transition temperatures, indicating different chain size. Concentration determinations with NaCl, saccharose and whey protein allow to identify the structural changes of the membranes regarding the glycerin content. Hence, sample M1 synthesized with the lowest glycerin concentration in the series, exhibit the higher retention of the penetrant molecule, particularly, the whey protein.

Acknowledgements

To the Vicerrectoria de Investigación y Estudios de Posgrado (VIEP-BUAP) by the financial support to carry out this research.

References

Bocourt-Povea, M., Cruz-Rigñack, J., Bada-Rivero, N., & Peniche-Covas, C. (2008). Síntesis y caracterización de hidrogeles biocompatibles interpenetrados de quitosana y poliacrilamida. *CENIC, Ciencias Químicas 39*, 70-74.

Bullón, J., Chaffaut, J. J., Belleville, M. P., Newman, R. D., & Ríos, G. M. (2001). Characterization and properties of supported protein membranes. *Separation Science and Technology 36*. https://doi.org/10.1081/SS-100107760

Buszard, D. (1984). Theoretical Aspects of Plasticisation. In: *PVC Tecnology*. Springer, Dordrecht. https://doi.org/10.1007/978-94-009-5614-8_5

Carmona-Gómez, L., Piovesana, A., Noreña, C., & Brandelli, A. (2018). Separation of polyphenolic compounds by ultrafiltration of bordo grape (*Vitis labrusca* var. Bordo) skin xtract. *Revista Mexicana de Ingeniería*

Química 17, 203-213. https://doi.org/10.24275/uam/izt/dcbi/revmexingquim/2018v17n1/Carmona

Chaudhary, D., Adhikari, B., & Kasapis, S. (2011). Glass-transition behaviour of plasticized starch biopolymer system modified. *Food Hydrocolloids 25*, 114-121. https://doi.org/10.1016/j.foodhyd.2010.06.002

Chen, X.-G., Zheng, L., Wang, Z., Lee, C., & Park, H.-J. (2002). Molecular affinity and permeability of different molecular weight chitosan membranes. *Journal of Agricultural and Food Chemistry 50*, 5915-5918. https://doi.org/10.1021/jf020151g

Chen, Z., Lou, J., Chen, X., Hang, X., Shen, F., & Yinhua, W. (2016). Fully recycling dairy wastewater by an integrated isoelectric precipitation−nanofiltration−anaerobic fermentation process. *Chemical Engineering Journal 283*, 476−485. https://doi.org/10.1016/j.cej.2015.07.086

Cui, Z., Xiang, Y., Si, Y., Yang, M., Zhang, Q., & Zhang. (2008). Ionic interaction between sulfuric acid and chitosan membranes. *Carbohydrate Polymers*, 111-116.

Feng , Z., Shao , Z., Yao , J., Huang , Y., & Chen, X. (2009). Protein adsorption and separation with chitosan-based amphoteric membranes. *Polymer 50*, 1257−1263.

Godwin, A. (2011). Plasticizers. In *Applied Plastics Engineering Handbook* (pp. 487−501). https://doi.org/10.1016/b978-1-4377-3514-7.10028-5

González-Valdez, J., Mayolo-Delosa, K., González-González, M., & Rito-Palomares, M. (2014). Trends in bioseparations. *Revista Mexicana de Ingeniería Química*, 19-27.

Han, Y.-J., Wang, K.-H., Lai, J.-Y., & Liu, Y.-L. (2014). Hydrophilic chitosan-modified polybenzoimidazole membranes for pervaporation dehydration of isopropanol aqueous solutions. *Journal of Membrane Science 463*, 17-23. https://doi.org/10.1016/j.memsci.2014.03.052

Ho, Y. & McKay, G. (1998). Comparison of chemisorption kinetic models applied to pollutant removal on various sorbents. Trans Chem., 76(Parte B). https://doi.org/10.1205/095758298529696

Kolesnyk, I., Konovalova , V., Kharchenko , K., Burban , Kujawa , J., & Kujawski, W. (2020). Enhanced transport and antifouling properties of polyethersulfone membranes modified with α-amylase incorporated in chitosan-based polymeric micelles. *Journal of Membrane Science*. https://doi.org/10.1016/j.memsci.2019.117605

Liu, H., Adhikari , R., Guo, Q., Adhikari, B., Liu, H., Adhikari, R., & Guo, Q. (2013). Preparation and characterization of glycerol plasticized (high-amylose) starch−chitosan films. *Journal of Food Engineering 16*, 588−597. https://doi.org/10.1016/j.jfoodeng.2012.12.037

López-Díaz, A., Ríos-Corripio, M., Ramírez-Corona, López-Malo, E., & Palou, E. (2018). Effect of short wave ultraviolet radiation on selected properties of edible films formulated with pomegranate juice and chitosan. *Revista Mexicana de Ingeniería Química 17*, 63-73. https://doi.org/10.24275/uam/izt/dcbi/revmexingquim/2018v17n1/Lopez

Marques, J. S., Changas, J. A., Fonseca, J. L., & Pereira, M. R. (2016). Comparing homogeneous and heterogeneous routes for ionic crosslinking of chitosan membranes. *Reactive and Functional Polymers 103*, 156−161. https://doi.org/10.1016/j.reactfunctpolym.2016.04.014

Martínez , A., Cortez , M., Ezquerra , J., Graciano , A., Rodríguez , Z., Castillo , M.,... Plascencia, M. (2010). Chitosan composite films: Thermal, structural, mechanical and antifungal Properties. *Carbohydrate Polymers 82*, 305-315.

Matta, C. F., Massa, L., Gubskaya, A. V., & Knoll, E. (2011). Can on table the logartithm ir the sine of a dimensioned quantity or a unit? Dimensional analysis involving transcendental functions. *Journal of Chemical Eduactaion 88*, 67-70. https://doi.org/10.1021/ed1000476

Mu, X.-T., Ju, X.-J., Zhang, L., Huang, X.-B., Liu, Z., Wang, W., ...Faraj, Y. (2019). Chitosan microcapsule membranes with nanoscale

thickness for controlled release of drugs. *Journal of Membrane Science*.

Neto, C., Giacometti, J., Job, A., Ferreira, F., Fonseca, J., & Pereira, M. (2005). Thermal analysis of chitosan based networks. *Carbohydrate Polymers 62*, 97-103. https://doi.org/10.1016/j.carbpol.2005.02.022

Núñez-Gastélum, J., Rodríguez-Núñez, J., de la Rosa, L., Díaz-Sánchez, A., Alvarez-Parrilla, Martínez-Martínez, A., & Villa-Lerma, G. (2018). Screening of the physical and structural properties of chitosan-polycaprolactone films added with *Moringa oleifera* leaf extract. *Revista Mexicana de Ingeniería Química 18*, 99-105. https://doi.org/10.24275/uam/izt/dcbi/revmexingquim/2019v18n1/Nunez

Perez-Escobar, L., Mosquera-Martinez, A., Ciro-Velasquez, H., Sepulveda-Valencia, J., & Vargas-Diaz, S. (2020). Obtention of a lactose hydrolysate from nanofiltration of sweet whey: characterization and process optimization. *Revista Mexicana de Ingeniería Química 19*, 445-453. https://doi.org/10.24275/rmiq/Proc649

Ramos-García, M., Bautista-Baños, S., & González-Soto, R. (2018). Physical properties of chitosan films with lemon essential oiladded and their impact on the shelf life of tomatoes (*Lycopersiconesculentum* L.). *Revista Mexicana de Ingeniería Química 17*, 1-11. https://doi.org/10.24275/uam/izt/dcbi/revmexingquim/2018v17n1/Bautista

Sajjan, A. M., Premakshi, H. G., & Kariduraganavar, M. Y. (2015). Synthesis and characterization of GTMAC grafted chitosan membranes for the dehydration of low water content isopropanol by pervaporation. *Journal of Industrial and Engineering Chemistry 25*, 151-161. https://doi.org/10.1016/j.jiec.2014.10.027

Scott, K. (1995). *Handbook of Industrial Membranes*. Elseiver.

Shahidi, F., Arachchi, J., & Jeon, Y. (1999). Food applications of chitin and chitosans. *Trends Food Sci. Technol 10*, 37-51.

Sivashankari , P., & Prabaharan , M. (2017). Deacetylation modification techniques of chitin and chitosan. *Chitosan Based Biomaterials 1*, 117-133. https://doi.org/10.1016/B978-0-08-100230-8.00005-4

Srinivasa, P. C., Ramesh, M. N., & Tharanathan, R. N. (2007). Effect of plasticizers and fatty acids on mechanical and permeability characteristics of chitosan films. *Food Hydrocolloids 21*, 1113-1122. https://doi.org/10.1016/j.foodhyd.2006.08.005

Tharanathan, R. N. (2013). Biodegradable films and composite coatings: past, present and future. *Trends in Food Science & Technology*, 14, 71-78. https://doi.org/10.1016/S0924-2244(02)00280-7

van Reis , R., & Zydney, A. (2007). Bioprocess membrane technology. *Journal of Membrane Science 297*, 16-50. https://doi.org/10.1016/j.memsci.2007.02.045

Wang, W., Bo, S., Li, & Qin, S. (1991). Determination of the Mark-Houwink equation for chitosans with different degrees of deacetylation. *International Journal of Biological Macromolecules 13*, 281−285.

Xi-Guang, C., Li, Z., Zhen, W., Chang-Yong, L., & Hyun-Jin, P. (2002). Molecular affinity and permeability of different molecular weight chitosan membranes. *J. Agric. Food Chem. 50*, 5915-5918. https://doi.org/10.1021/jf020151g

Xin-Ping, W., Zhi-Quan, S., Fu-Yao, Z., & Yi-Feng, Z. (1996). A novel composite chitosan membrane for the separation of alcohol-water mixtures. *Journal Membranes Sci 196*, 191-198. https://doi.org/10.1016/0376-7388(96)00157-3

Zhao Wang, Q., Guang Chen, X., Liu, N., Xi Wang, S., Sheng Liu, C., Hong Meng, X., & Guang Liu, C. (2006). Protonation constants of chitosan with different molecular weight and degree of deacetylation. *Carbohydrate Polymers 65*, 194−201. https://doi.org/10.1016/j.carbpol.2006.01.001

Zhu, J., Tian, M., Zhang, Y., Zhang, H., & Liu, J. (2015). Fabrication of a novel "loose" nanofiltration membrane by facile blending with Chitosan−Montmorillonite nanosheets for dyes purification. *Chemical Engineering Journal 265*, 184-193. https://doi.org/10.1016/j.cej.2014.12.054